Langmuir

Letter

pubs.acs.org/Langmuir

Citrate-Stabilized Gold Nanorods

Jonathan G. Mehtala, Dmitry Y. Zemlyanov, Joann P. Max, Naveen Kadasala, Shou Zhao, and Alexander Wei*

Department of Chemistry, Purdue University, 560 Oval Drive, West Lafayette, Indiana 47907-2084, United States

Supporting Information

ABSTRACT: Stable aqueous dispersions of citrate-stabilized gold nanorods (cit-GNRs) have been prepared in scalable fashion by surfactant exchange from cetyltrimethylammonium bromide (CTAB)-stabilized GNRs, using polystyrenesulfonate (PSS) as a detergent. The surfactant exchange process was monitored by infrared spectroscopy, surface-enhanced Raman scattering (SERS), and X-ray photoelectron spectroscopy (XPS). The latter established the quantitative displacement of CTAB (by PSS) and of PSS (by citrate). The Cit-GNRs are indefinitely stable at low ionic strength, and are conducive to further ligand exchange without loss of dispersion stability. The reliability of the surface exchange process supports the systematic analysis of ligand structure on the hydrodynamic size of GNRs, as described in a companion paper.

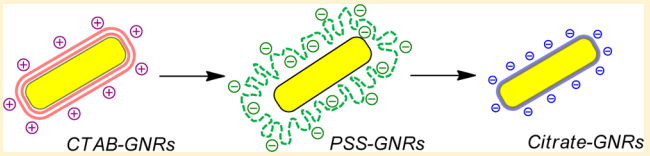

INTRODUCTION

Gold nanorods (GNRs) are anisotropic particles whose surface plasmon modes can be tuned as a function of aspect ratio, with optical resonances ranging from visible to near-infrared wavelengths.[1,2] GNRs have been investigated as contrast agents for optical biomedical imaging modalities such as optical coherence tomography and photoacoustic tomography; they are also capable of producing linear and two-photon excited luminescence, with detection limits at the single-particle level.[3] The large absorption cross sections of GNRs can also generate localized photothermal effects,[4] with application toward the release of molecular cargo[5−7] and hyperthermic effects on diseased cells and tissues.[3,8−11] These attributes have sparked a global effort to develop GNRs into theranostic agents for nanomedicine.[1]

One hurdle in the scalable manufacturing of GNR-based materials is the efficient exchange and removal of cetyltrimethylammonium bromide (CTAB), a micellar surfactant used in the batch synthesis of GNRs.[2] CTAB is cationic and moderately cytotoxic (although not insupportably so),[12,13] most of which can be removed by multiple washes and exchanges with chemisorptive surfactants (e.g., PEGylated thiols or dithiocarbamates),[12,14,15] phospholipids,[16] or other surface-active agents.[17,18] However, CTAB-coated GNR dispersions are frequently destabilized during surfactant exchange, resulting in partial aggregation and low recovery yields. Furthermore, ligand-modified GNRs are often contaminated with residual CTAB, which can induce nonspecific protein adsorption and cell uptake under physiological conditions,[12] or produce surface charge defects in materials applications. We have previously shown that CTAB-depleted GNR dispersions can be prepared when using sodium polystyrenesulfonate (Na-PSS) as a mild detergent;[17] nevertheless, the stability of such suspensions remains capricious in subsequent manipulations. We thus sought to develop a practical method for producing CTAB-free GNR dispersions that would be universally compatible with surface conjugation protocols.

In this Letter we describe an efficient method for converting CTAB-stabilized GNRs into citrate-stabilized GNRs (cit-GNRs) via intermediate treatment with PSS. The surface exchange process was monitored in stages by X-ray photoelectron spectroscopy (XPS), an invaluable tool for quantitative elemental analysis of surface adsorbates, as well as by attenuated total reflectance infrared (ATR-IR) spectroscopy and surface-enhanced Raman scattering (SERS). Our analyses indicate that CTAB removal by PSS treatment is highly efficient, as is the subsequent displacement of PSS by citrate. The cit-GNRs are fully dispersible in low-salt solutions, and are easily functionalized by further ligand exchange (discussed in a companion article).[19]

EXPERIMENTAL SECTION

A six-stage protocol was developed to convert CTAB-GNRs (68 × 26 nm, λ_{LPR} = 713 nm) into cit-GNRs, using standard ultrafiltration and centrifugation equipment. CTAB-GNRs were prepared on a gram scale by the method described by Khanal and Zubarev,[20] and diluted 4-fold to prevent premature flocculation of CTAB-GNRs during the initial purification stages. In a typical process, a suspension of GNRs (optical density (O.D.) = 3.2) stabilized in 25 mM CTAB was concentrated by stirred ultrafiltration to remove excess surfactant, then diluted with deionized water (Stage 1; Figure 1). The GNRs were then subjected to three cycles of centrifugation and redispersion (C/R) to deplete CTAB to trace levels, using 0.15 wt % Na-PSS (M_w = 70 kDa; Stages 2−4). We note that the residual CTAB in the PSS-stabilized GNR suspension after Stage 4 is <1 μM based on simple dilution factors; however, the free CTAB concentration is likely even lower due to its favorable adsorption to PSS.[21] The PSS-GNRs were then subjected to two additional C/R cycles using 5 mM sodium citrate

Received: July 25, 2014
Revised: September 23, 2014
Published: September 25, 2014

   dx.doi.org/10.1021/la5029542 | Langmuir 2014, 30, 13727−13730

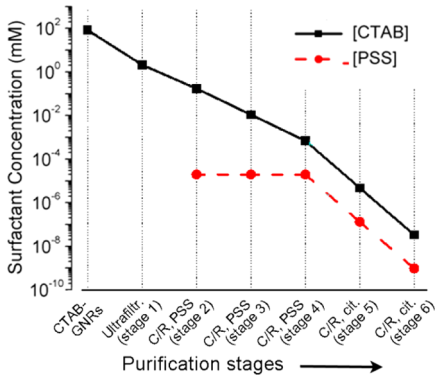

Figure 1. Process flow diagram for converting CTAB-GNRs into cit-GNRs by ultrafiltration (stage 1) with successive C/R cycles using 0.15 wt % Na-PSS (stages 2–4) and 5 mM Na_3-cit (stages 5 and 6), with estimated surfactant concentrations after each stage.

(Stages 5 and 6) for exchange with PSS, yielding stable dispersions of cit-GNRs. A complete procedure with exact volumes and concentrations is provided in the Supporting Information.

RESULTS AND DISCUSSION

The conversion of CTAB-GNRs into cit-GNRs was achieved with an overall efficiency of 75–85%, based on initial and final O.D. values of the GNR dispersions. The main source of loss is due to incomplete recovery of GNRs during the first two C/R cycles. Absorption spectroscopy and transmission electron microscopy (TEM) analysis of the citrate-stabilized GNRs indicated essentially no changes in optical resonance (λ_{max} = 710 nm; Figure 2) or size distribution (Figure S1, Supporting

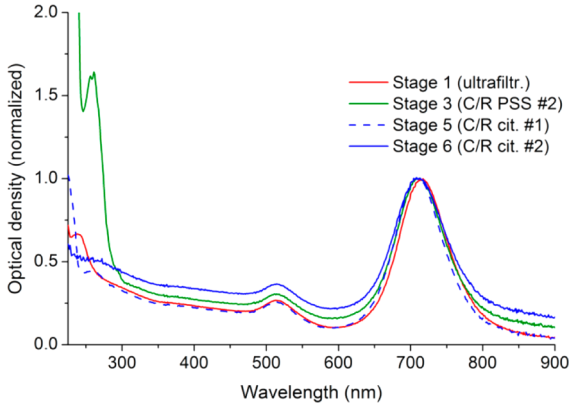

Figure 2. Normalized absorption spectra of GNR dispersions after ultrafiltration (Stage 1, red), C/R cycles with Na-PSS (Stage 3, green), and C/R cycles with Na_3-cit (Stages 5 and 6, blue).

Information). On the other hand, the exchange of PSS to citrate was readily discernible by electrokinetic measurements: the zeta potential of GNRs in dilute Na-PSS solution (0.25 mg/mL, pH 5) was −55.6 ± 8.3 mV, while that of cit-GNRs in dilute phosphate buffered solution (PBS) adjusted to pH 9.5 (I ∼ 8.2 mM) was less negative (mean −26.9 ± 13.2 mV; mode −21.1 ± 7.1 mV). The cit-GNR suspensions are stable for months at low ionic strength but aggregate if dispersed in highly saline solutions (also see below), and thus behave similarly as other citrate-stabilized Au nanoparticles.

The incubation of GNRs with 70-kDa Na-PSS (minimum 1 h, prior to each C/R step) is essential for producing well-dispersed cit-GNRs. Previous studies in our laboratory have established that PSS is useful as a detergent for removing residual CTAB from GNR dispersions, below the level of observable cytotoxicity.[17] However, Na-PSS by itself is not suitable as a peptizing agent: it adsorbs weakly onto GNR surfaces in the absence of CTAB, resulting in metastable dispersions whose relative stability depends on polymer concentration, suggestive of depletion effects.[22,23] GNRs cleansed with PSS can be stabilized afterward by introducing surface-active agents that do not associate strongly with the polyelectrolyte. In this regard, polyanions with moderate binding activity such as citrate are ideal for surface exchange; the PSS is gently displaced from the GNRs while maintaining a negative zeta potential during the exchange process. Nonionic, hydrophilic surfactants can also be used to displace PSS from GNR surfaces,[17] but the efficiency of exchange depends on the specific qualities of the surface-active agent. Attempts to treat CTAB-GNRs directly with citrate without Na-PSS cleansing invariably led to rapid aggregation, regardless of surfactant concentrations (Figure S2, Supporting Information). This is not surprising, as the citrate anions neutralize the positive surface charge supported by the resident CTAB layer, resulting in particle destabilization prior to complete ligand exchange. It has been reported that citrate preferentially adsorbs onto the ends of CTAB-GNRs, resulting in their end-to-end aggregation.[24]

The ligand exchange process from Stage 3 (PSS wash #2) to Stage 6 (citrate wash #2) was evaluated by XPS, based on the binding energies (B.E.) of various atomic species (Table 1 and Figure 3). The XPS signal corresponding to bromine (Br 3d; 68.5 eV) could not be detected even at Stage 3, whereas that of nitrogen (N 1s; 401 eV) was reduced below the limit of detection by Stage 5, establishing the essentially complete displacement of CTAB from the GNR surfaces. The XPS signals for carbon (C 1s), oxygen (O 1s), sodium (Na 1s), and sulfur (S 2p) were also greatly reduced upon washing with 5 mM citrate (Stage 5), indicating the gross displacement of Na-PSS from the GNR surfaces (Figure 3a). The S 2p signal was almost completely gone by the second citrate wash (Stage 6), and below trace levels in the supernatant. High-resolution analysis of the C 1s region further revealed that citrate exchange was accompanied by a change in the population of carbon subtypes, with a reduction in hydrocarbon species (C–H/C–C; B.E. = 284.8 eV) and an increase in the density of carboxyl groups (C(=O)O; B.E. = 288.2 eV), corresponding with the adsorption of citrate (Figure 3b).

It is worth noting that the XPS spectra also indicated the significant presence of silver (Ag 3d; ca. 25% versus Au 4f), which remained approximately constant throughout the ligand exchange process. $AgNO_3$ is used as an additive in the seeded growth of GNRs,[20,25,26] and has been postulated to contribute toward shape control by its selective deposition onto longitudinal facets.[27] This notion has recently been brought into question by high-resolution TEM imaging using energy dispersive X-ray spectroscopy, which indicated the distribution of Ag over the entire GNR surface.[28] Regardless of mechanism, the intensity of the Ag 3d XPS signal in our study also suggests that the deposited Ag is mostly localized near the GNR surface.

The ligand exchange process was also characterized by ATR-IR spectroscopy and SERS, to identify the molecular species associated with the GNR samples (Figures S3 and S4, Supporting Information). IR analysis of pelleted GNR samples from Stages 1, 3, and 4 confirmed the presence (and depletion) of CTAB and PSS, with the former producing strong bands

dx.doi.org/10.1021/la5029542 | Langmuir 2014, 30, 13727–13730

Table 1. XPS Analysis of GNR Samples at Different Purification Stages

element (B.E., eV)[c]	Stage 3[a] (PSS #2)	bkgrnd[b] (PSS #2)	Stage 4[a] (PSS #3)	bkgrnd[b] (PSS #3)	Stage 5[a] (Cit. #1)	bkgrnd[b] (Cit. #1)	Stage 6[a] (Cit. #2)	bkgrnd[b] (Cit. #2)
C 1s (283)	210	93.8	205	67.6	8.00	9.27	6.44	1.04
N 1s (401)	1.51	--	1.28	--	0.03[d]	--	0.03[d]	--
O 1s (530)	80.3	39.3	86.7	32.4	4.14	11.7	4.54	3.02
Na 1s (1069)	21.8	13.3	26.3	13.2	1.28	4.47	1.79	0.60
S 2p (167)	24.1	11.4	26.6	9.19	0.47	0.47	0.09	<0.03[d]
Ag 3d (366)	0.25	--	0.26	--	0.28	--	0.26	--
Si 2s (101)	--	1	--	1	--	1	--	1
Au 4f (82)	1	--	1	--	1	--	1	--

[a]Signals from pelleted GNR samples, normalized to Au 4f peak area. [b]Signals from supernatant of GNR samples, normalized to Si 2s peak area. [c]Binding energies from survey XPS spectra. [d]At or below limit of detection.

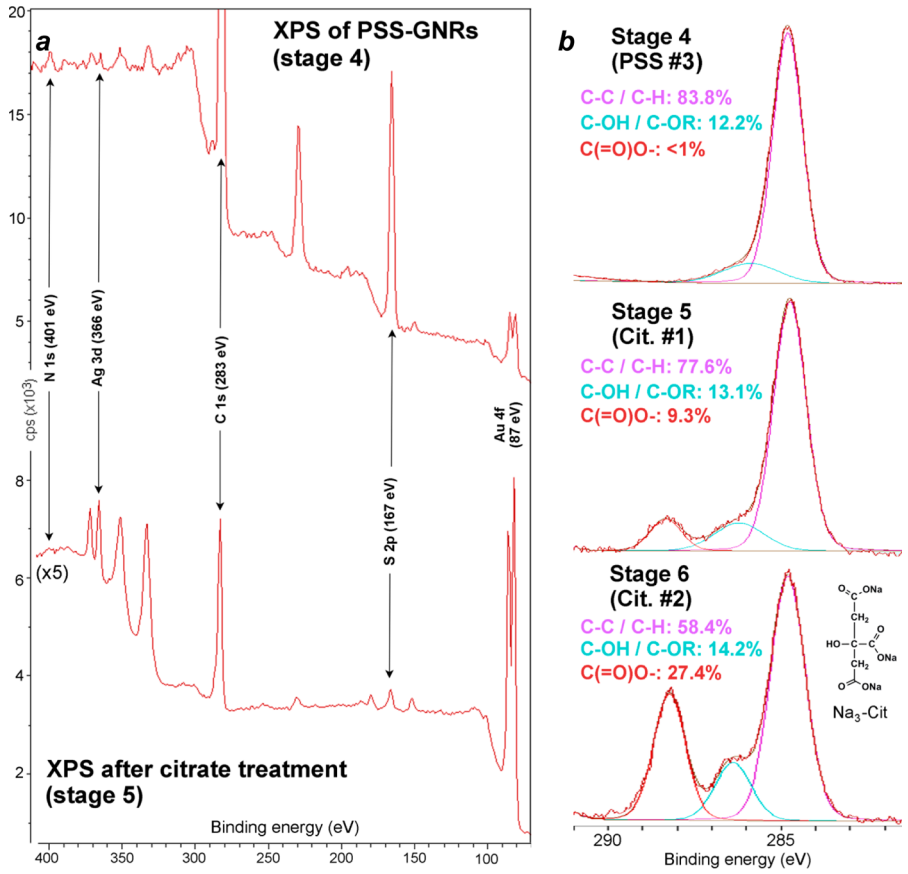

Figure 3. (a) Survey XPS spectra acquired from pelleted GNR samples after Stage 4 (PSS wash #3) and Stage 5 (Citrate wash #1; 5× magnification), indicating the disappearance of the N 1s signal. (b) High-resolution (regional) XPS spectra of the C 1s region, indicating relative changes in carbon subtype after treatment with citrate.

associated with sp^3 C−H stretching (2800−2900 cm^{-1}), $-CH_3$ deformation (1450−1480 cm^{-1}), and C−N stretching (900−950 cm^{-1}), and the latter producing peaks associated with the $-SO_3^-$ group (1020−1200 cm^{-1}).[29] PSS displacement by citrate anions produced additional spectral changes, dominated by CO_2^- stretching (1575 cm^{-1}) and $-CH_2$ deformation (1390 cm^{-1}). SERS analysis also confirmed that PSS was adsorbed onto GNRs by the enhanced SO_3^- Raman signal, but was displaced after two washes with Na_3-cit. Overall, these vibrational analyses further support the conclusions drawn from the XPS data.

Citrate-stabilized Au nanoparticles are widely appreciated for their versatility in surface modification protocols, with minimal interference by the displaced electrolyte.[30] We conducted a preliminary survey of cit-GNRs dispersed in different aqueous solutions, to determine their relative stability during surface functionalization. Dispersions of Cit-GNRs are stable in 10 mM sodium citrate (I = 60 mM), but slowly aggregate in standard PBS (I ~160 mM) or 1 M NaCl. However, cit-GNRs treated with nonionic surfactants such as Tween-20, chemisorptive surfactants such as thiolated polyethylene glycol, or serum proteins such as albumin all form stable dispersions in PBS. Such coated GNRs have been characterized and are further described in our companion paper.[19]

■ OUTLOOK

The protocol described above is a mild and general approach for depleting CTAB and other cationic surfactants from

dx.doi.org/10.1021/la5029542 | Langmuir 2014, 30, 13727−13730

aqueous nanoparticle suspensions, allowing their clean exchange with citrate ions. The citrate-stabilized GNRs are compatible with surface conjugation chemistries commonly applied to metal colloids, and provide a reliable platform for making rational changes in chemical and biological properties as a function of surface modification.[19]

■ ASSOCIATED CONTENT

Supporting Information

Detailed description of surfacant exchange protocol; additional characterization data (TEM optical absorbance, ATR-IR, SERS). This material is available free of charge via the Internet at http://pubs.acs.org.

■ AUTHOR INFORMATION

Corresponding Author

*Tel.: (765) 494-5257; E-mail: alexwei@purdue.edu.

Notes

The authors declare no competing financial interest.

■ ACKNOWLEDGMENTS

This work was supported by the National Cancer Institute (RC1 CA-147096), the Birck Nanotechnology Center, and the Purdue University Center for Cancer Research (P30 CA023168). We gratefully acknowledge Eugene Zubarev (Rice University) for his generous contribution of gold nanorods to this project.

■ REFERENCES

(1) Wei, A.; Leonov, A. P.; Wei, Q. S. Gold Nanorods: Multifunctional Agents for Cancer Imaging and Therapy. In *Cancer Nanotechnology: Methods and Protocols*; Grobmyer, S. R., Moudgil, B. M., Eds.; Humana Press, Inc: Totowa, NJ, 2011; Vol. *624*, pp 119−130.

(2) Dreaden, E. C.; Alkilany, A. M.; Huang, X.; Murphy, C. J.; El-Sayed, M. A. The Golden Age: Gold Nanoparticles for Biomedicine. *Chem. Soc. Rev.* **2012**, *41*, 2740−2779.

(3) Tong, L.; Wei, Q.; Wei, A.; Cheng, J.-X. Gold Nanorods as Contrast Agents for Biological Imaging: Surface Conjugation, Two-Photon Luminescence, and Photothermal Effects. *Photochem. Photobiol.* **2009**, *85*, 21−32.

(4) Chou, C.-H.; Chen, C.-D.; Wang, C. R. C. Highly Efficient, Wavelength-Tunable, Gold Nanoparticle Based Optothermal Nanoconvertors. *J. Phys. Chem. B* **2005**, *109*, 11135−11138.

(5) Yamashita, S.; Fukushima, H.; Niidome, Y.; Mori, T.; Katayama, Y.; Niidome, T. Controlled-Release System Mediated by a Retro Diels-Alder Reaction Induced by the Photothermal Effect of Gold Nanorods. *Langmuir* **2011**, *27*, 14621−14626.

(6) Wijaya, A.; Schaffer, S. B.; Pallares, I. G.; Hamad-Schifferli, K. Selective Release of Multiple DNA Oligonucleotides from Gold Nanorods. *ACS Nano* **2009**, *3*, 80−86.

(7) Kuo, T.-R.; Hovhannisyan, V. A.; Chao, Y.-C.; Chao, S.-L.; Chiang, S.-J.; Lin, S.-J.; Dong, C.-Y.; Chen, C.-C. Multiple Release Kinetics of Targeted Drug from Gold Nanorod Embedded Polyelectrolyte Conjugates Induced by Near-Infrared Laser Irradiation. *J. Am. Chem. Soc.* **2010**, *132*, 14163−14171.

(8) Dickerson, E. B.; Dreaden, E. C.; Huang, X.; El-Sayed, I. H.; Chu, H.; Pushpanketh, S.; McDonald, J. F.; El-Sayed, M. A. Gold Nanorod Assisted Near-Infrared Plasmonic Photothermal Therapy (PPTT) of Squamous Cell Carcinoma in Mice. *Cancer Lett.* **2008**, *269*, 57−66.

(9) von Maltzahn, G.; Park, J.-H.; Agrawal, A.; Bandaru, N. K.; Das, S. K.; Sailor, M. J.; Bhatia, S. N. Computationally Guided Photothermal Tumor Therapy Using Long-Circulating Gold Nanorod Antennas. *Cancer Res.* **2009**, *69*, 3892−3900.

(10) Choi, W. I.; Kim, J.-Y.; Kang, C.; Byeon, C. C.; Kim, Y. H.; Tae, G. Tumor Regression in Vivo by Photothermal Therapy Based on Gold-Nanorod-Loaded, Functional Nanocarriers. *ACS Nano* **2011**, *5*, 1995−2003.

(11) Mehtala, J. G.; Torregrosa-Allen, S.; Elzey, B. D.; Jeon, M.; Kim, C.; Wei, A. Synergistic Effects of Cisplatin Chemotherapy and Gold Nanorod-Mediated Hyperthermia on Ovarian Cancer Cells. *Nanomedicine* **2014**, *9*, 1939−1955.

(12) Huff, T. B.; Hansen, M. N.; Zhao, Y.; Cheng, J.-X.; Wei, A. Controlling the Cellular Uptake of Gold Nanorods. *Langmuir* **2007**, *23*, 1596−1599.

(13) Alkilany, A. M.; Nagaria, P. K.; Hexel, C. R.; Shaw, T. J.; Murphy, C. J.; Wyatt, M. D. Cellular Uptake and Cytotoxicity of Gold Nanorods: Molecular Origin of Cytotoxicity and Surface Effects. *Small* **2009**, *5*, 701−708.

(14) Liao, H.; Hafner, J. H. Gold Nanorod Bioconjugates. *Chem. Mater.* **2005**, *17*, 4636−4641.

(15) Kinnear, C.; Dietsch, H.; Clift, M. J. D.; Endes, C.; Rothen-Rutishauser, B.; Petri-Fink, A. Gold Nanorods: Controlling Their Surface Chemistry and Complete Detoxification by a Two-Step Place Exchange. *Angew. Chem., Int. Ed.* **2013**, *52*, 1934−1938.

(16) Takahashi, H.; Niidome, Y.; Niidome, T.; Kaneko, K.; Kawasaki, H.; Yamada, H. Modification of Gold Nanorods Using Phosphatidylcholine to Reduce Cytotoxicity. *Langmuir* **2006**, *22*, 2−5.

(17) Leonov, A. P.; Zheng, J.; Clogston, J. D.; Stern, S. T.; Patri, A. K.; Wei, A. Detoxification of Gold Nanorods by Treatment with Polystyrenesulfonate. *ACS Nano* **2008**, *2*, 2481−2488.

(18) Indrasekara, A. S. D. S.; Wadams, R. C.; Fabris, L. Ligand Exchange on Gold Nanorods: Going Back to the Future. *Part. Part. Syst. Charact.* **2014**, *31*, 819−838.

(19) Mehtala, J. G.; Wei, A. Nanometric Resolution in the Hydrodynamic Size Analysis of Ligand-Stabilized Gold Nanorods. *Langmuir* **2014**, DOI: 10.1021/la502955h.

(20) Khanal, B. P.; Zubarev, E. R. Rings of Nanorods. *Angew. Chem., Int. Ed.* **2007**, *46*, 2195−2198.

(21) Semchyschyn, D. J.; Carbone, M. A.; Macdonald, P. M. Anionic Polyelectrolyte Binding to Mixed Cationic-Zwitterionic Surfactant Micelles: A Molecular Perspective from ^{2}H NMR Spectroscopy. *Langmuir* **1996**, *12*, 253−260.

(22) Napper, D. H. *Polymer Stabilization of Colloid Dispersions*; Academic: New York, 1983.

(23) Takeda, S.-i.; Tobori, N.; Sugawara, H.; Furusawa, K. Dynamic Electrophoresis. In *Electrical Phenomena at Interfaces: Fundamentals, Measurements, and Applications*, 2nd ed.; Ohshima, H.; Furusawa, K., Eds.; CRC Press: Boca Raton, FL, 1998; pp 273−304.

(24) Kawamura, G.; Yang, Y.; Nogami, M. End-to-End Assembly of CTAB-Stabilized Gold Nanorods by Citrate Anions. *J. Phys. Chem. C* **2008**, *112*, 10632−10636.

(25) Nikoobakht, B.; El-Sayed, M. A. Preparation and Growth Mechanism of Gold Nanorods (NRs) Using Seed-Mediated Growth Method. *Chem. Mater.* **2003**, *15*, 1957−1962.

(26) Sau, T. K.; Murphy, C. J. Seeded High Yield Synthesis of Short Au Nanorods in Aqueous Solution. *Langmuir* **2004**, *20*, 6414−6420.

(27) Liu, M. Z.; Guyot-Sionnest, P. Mechanism of Silver(I)-Assisted Growth of Gold Nanorods and Bipyramids. *J. Phys. Chem. B* **2005**, *109*, 22192−22200.

(28) Jackson, S. R.; McBride, J. R.; Rosenthal, S. J.; Wright, D. W. Where's the Silver? Imaging Trace Silver Coverage on the Surface of Gold Nanorods. *J. Am. Chem. Soc.* **2014**, *136*, 5261−5263.

(29) Lin-Vien, D.; Colthup, N. B.; Fateley, W. G.; Grasselli, J. G. *The Handbook of Infrared and Raman Characteristic Frequencies of Organic Molecules*, 2nd ed.; Academic Press: San Diego, CA, 1991.

(30) Hayat, M. A. *Colloidal Gold: Principles, Methods, and Applications*; Academic Press: San Diego, CA, 1989; Vol. *1*.